

ONLINE SUPPLEMENT

MATERIALS AND METHODS

Materials: ELISA kits to measure human MMP-9, murine Mmp-9, murine interleukin-6 (Il-6), murine chemokine C-C motif ligand-5 (Ccl-5), murine interleukin-10 (Il-10), murine interleukin-1 beta (Il-1 β), murine Ccl-2, murine tumor necrosis factor- α (Tnf- α), murine transforming growth factor- β (Tgf- β), and murine E-cadherin were obtained from R & D Systems (Minneapolis, MN). ELISA kits to quantify murine granulocyte colony stimulating factor (G-csf), murine macrophage inflammatory protein-1 α (Ccl-3), murine chemokine C-X-C motif ligand-2 (Cxcl-2), and murine keratinocyte-derived chemokine (Cxcl-1) were purchased from Peprotech (Rocky Hill, NJ). ELISA kits to measure murine interferon- α (Ifn- α) and murine Ifn- γ were purchased from Affymetric eBioscience (San Diego, CA). ELISA kits to quantify murine Ifn- β were purchased from PBL Assay science (Piscataway, NJ). The murine Cxcl-6 ELISA kit was purchased from MyBiosource (San Diego, CA). All ELISA kits detect full length chemokine and/or cytokines. Human MMP-9 and GM6001 were purchased from EMD Millipore (Billerica, MA). 1,10-phenanthroline (OP) was purchased from Sigma-Aldrich (St Louis, MO). All antibodies used for flow cytometry immunostaining were purchased from Biolegend (San Diego, CA).

Specificity of the MMP-9 and Mmp-9 ELISA kits. The human MMP-9 kit (R & D Systems, Minneapolis, MN) detects pro-MMP9 (92 kDa), active MMP-9 (82 kDa) and MMP-9/neutrophil gelatinase-associated lipocain heterodimers (107 kDa). The ELISA kit for murine Mmp-9 (R & D Systems, Minneapolis, MN) detects pro-Mmp-9, active-Mmp-9 and Mmp-9/Timp complexes.

Human blood sample processing: Venous blood was collected and centrifuged at 224 \times g for 10 min at 4°C within 2 h of collection. The serum was separated and stored at -80°C for analysis.

Virus stocks: Madin-Darby canine kidney (MDCK, CCL-34) cells (American Tissue Culture Collection, Manassus, VA) were maintained in minimum essential medium (MEM) supplemented with L-glutamine, Earle's salts, 10% fetal bovine serum, and 100 U/mL penicillin, 100 µg/mL streptomycin and 0.25 µg/ml amphotericin B (ThermoFisher Scientific, Waltham, MA). The pandemic IAV strain, influenza A/California/07/2009 H1N1 (H1N1), was obtained from Centers for Disease Control (Atlanta, GA), propagated in MDCK cells, and used to infect mice. Titers of stock were measured using a standard plaque assay on 6-well plates of confluent monolayers of MDCK cells using a 0.6% Avicel CL-611 solution (FMC Corporation, Philadelphia, PA) containing 3 µg/mL of trypsin solution treated with 1-tosylamido-2-phenylethyl chloromethyl ketone (Worthington Biochemical Corporation, Lakewood, NJ).

Animals: All studies conducted on mice were approved by the Institutional Care and use Committees at Brigham and Women's Hospital and the Lovelace Respiratory Research Institute. Colonies of WT and *Mmp9*^{-/-} mice both in a pure C57BL/6 background were housed under identical conditions in a pathogen-free barrier facility, and provided with filtered air through separate duct system to Tecniplast cages, and exposed to 12 h light and dark cycles. Mice were fed PicoLab® Rodent Diet 20 (information available at: <http://www.labdiet.com>). Any WT mice that were purchased from Jackson Lab (Bar Harbor, ME) were co-housed with sex- and age-matched *Mmp9*^{-/-} mice under identical conditions for at least 10 days before being studied in experiments. *Mmp9*^{-/-} mice (backcrossed to the C57BL/6 strain for 10 generations) were generated as described previously (1). *Mmp9*^{-/-} mice have normal lifespan, and lung development, and no abnormalities in the lung have been identified in the unchallenged state (2). The genotypes of the mice were confirmed using PCR-based protocols performed on genomic DNA extracted from tail biopsies. Male and female WT and *Mmp9*^{-/-} mice were used in all experiments, and age- and sex-matched mice were randomized to experimental groups by an individual that was not involved in the conduct of the experiments.

Murine blood sample processing: Blood samples were obtained from WT mice via cardiac puncture. Blood was collected and allowed to clot on ice for 20 min, and was then centrifuged (at 500 g for 5 min). Serum was removed and stored at -80°C for analysis. Serum Mmp-9 levels were quantified using an ELISA kit (Cusabio, Hubei Providence, China).

Generation of *Mmp9* bone marrow (BM) chimeric mice: Unchallenged C57BL/6 WT and *Mmp9*^{-/-} mice were lethally irradiated twice, four hours apart, using a radiation dose of 450 centigray using a ¹³⁷Cesium source (3,4). After the second irradiation, mice received two million BM-derived cells in 50 µl of endotoxin-free normal saline via tail vein a injection. Four groups of *Mmp9*^{-/-} BM chimeras were generated by transplanting: 1) WT BM into WT recipients; 2) WT BM into *Mmp9*^{-/-} recipients; 3) *Mmp9*^{-/-} BM into WT recipients; and 4) *Mmp9*^{-/-} BM into *Mmp9*^{-/-} recipients. After 10 weeks of BM engraftment, mice were infected with a LD₈₀ inoculum of A/California/07/2009 H1N1 strain by the intranasal route. Survival was monitored twice daily and body weight was measured daily. Mice exhibiting loss of body weight > 20% of baseline or any other significant clinical signs of impending mortality were humanely euthanized.

Specificity of the MMP-9 and *Mmp-9* ELISA kits. The ELISA kit for measuring human MMP-9 levels (purchased from R & D Systems, Minneapolis, MN) detects pro-MMP9 (92 kDa), active MMP-9 (82 kDa) and MMP-9/neutrophil gelatinase-associated lipocain heterodimers (107 kDa). The ELISA kit for measuring murine MMP-9 levels (purchased from R & D Systems, Minneapolis, MN) detects pro-Mmp-9, active-Mmp-9 and Mmp-9/Timp complexes.

Specificity of the ELISA kits used to quantify lung levels of murine chemokine and cytokines: The kits for measuring mediators of inflammation were purchased from the following vendors, and details of the sequences of the mediators that were used to generate the antibodies using in the kits are provided. It is not clear whether any of these kits detects mediators that have undergone proteolytic processing in vivo.

Ccl-5 (R&D Systems, Minneapolis, MN): This kit was developed using *E. coli*-derived mouse recombinant Ser24-Ser91 Ccl-5. Ccl-2 (R&D Systems): this kit was developed using *E. coli*-derived Gln24-Arg96 Ccl-2 (Accession # Q5SVU3). Il-6 (R&D Systems): Il-6: this kit was developed against *E. coli*-derived Phe25-Thr211 Il-6 (Accession # P08505). Tnf- α (R&D Systems): this kit was developed using *E. coli*-derived Leu80-Leu235 Tnf- α (Accession # P06804). Cxcl-1 (PeproTech, Rocky Hill, NJ): this kit was developed against *E. coli*-derived Cxcl-1 (Accession # P12850). Ccl-3 (PeproTech): this kit was developed against *E. coli*-derived Ccl-3 (Accession # P10855). Cxcl-2 (PeproTech): this kit was developed against *E. coli*-derived Cxcl-2 (Accession # P10889). Tgf- β (R&D Systems): this kit was developed using Chinese Hamster Ovary CHO-derived Ala279-Ser390 Tgf- β (Accession # P01137). Il-10 (R&D Systems): this kit was developed against *E. coli*-derived Ser19-Ser178 Il-10 (Accession # NP_034678). Il-1 β (R&D Systems): this kit was developed against *E. coli*-derived Val118-Ser269 Il-1 β (Accession # NP_032387). G-csf (PeproTech): this kit was developed against *E. coli*-derived G-csf (Accession # P01587). Cxcl-6 (MyBiosource): this kit was developed against recombinant murine Gcp-2 (Accession #P80163.1). Ifn- α (Affymetrix eBioscience, San Diego, CA): this kit was developed against full length natural and recombinant murine Ifn- α . Ifn- β (PBL Assay Science, Piscataway, NJ): this kit was developed against full length natural and recombinant mouse Ifn- β . Ifn- γ (Affymetrix eBioscience): this kit was developed using NIH standard (Lot Gg02-901-533) Ifn- β .

Immunofluorescence staining of lung sections for Mmp-9: Formalin-fixed lung sections from mice were double immunostained for Mmp-9 and markers of epithelial cells (pancytokeratin), macrophages (Mac3), PMN (myeloperoxidase), or CD8⁺ T cells (CD8), or CD4⁺ T cells (CD4). Briefly, lung sections were immunostained with rabbit anti-murine Mmp-9 IgG (Abcam, Cambridge, MA) followed by goat anti-rabbit (Fab)₂ conjugated to Alexa-488.

Lung sections were also immunostained with the following antibodies: 1) mouse anti-murine pancytokeratin IgG2a (Sigma-Aldrich, St. Louis, MO) followed by goat anti-murine IgG conjugated to Alexa-546; 2) rat anti-murine MAC-3 IgG (BD Bioscience, San Jose, CA) followed by goat anti-rat IgG conjugated to Alexa-546; 3) goat anti-murine myeloperoxidase IgG (R&D systems, Minneapolis, MN) followed by rabbit anti-goat IgG conjugated to Alexa-546; 4) rat anti-murine CD45R IgG2a (Biolegend, San Diego, CA) followed by goat anti-rat IgG conjugated to Alexa-546; or 5) goat anti-murine CD4 IgG (Santa-Cruz, Dallas, TX) followed by rabbit anti-goat IgG conjugated to Alexa-546. All secondary antibodies were obtained from Invitrogen (Carlsbad, CA). Isotype-matched non-immune rabbit, rat, murine, or goat IgGs were used as control primary antibodies. Lung sections were counterstained with 4',6-diamidino-2-phenylindole (DAPI). Images of the immuno-stained lung sections were captured and analyzed using a confocal microscope (Olympus Corporation, Center Valley, PA). Confocal micrographs were recorded under fluorescence imaging mode in which cells were exposed to 488, and 570 nm light attenuated by an acusto-tunable optical filter.

Murine lung viral titers:

Viable viral titers: Pulmonary tissue (~80 mg/mouse) was homogenized in serum-free media using a TissueLyser Homogenizer (Qiagen Inc. Valencia, CA). Samples were centrifuged at 850 x *g* for 5 min at 4°C and supernatants stored at -80°C. Viral titers were measured using a modified foci determination assay on 96-well plates of confluent monolayers of MDCK cells as described for standard plaque assays, except that IAV titers were measured with an immunostaining procedure. Briefly, fixed cells were incubated with 0.3 % H₂O₂ in absolute methanol for 30 min, washed in PBS, and blocked in PBS containing 5% non-fat dry (NFD) milk for 30 min at room temperature. Cells were incubated with primary antibody to influenza nucleoprotein (MAB8257; EMD Millipore, Temecula, CA) at a 1:1000 dilution in the PBS containing NFD milk for 45 min at room temperature. Cells were washed 5 times in PBS and

then incubated with HRP-labelled goat anti-murine IgG (ab6789; Abcam, Cambridge, MA) at a 1:1000 dilution in PBS containing NFD milk for 45 min at room temperature. Cells were washed in PBS containing 0.05% Tween-20, and then washed 4 times in PBS. Staining for foci was completed with the use of the ImmPACT™ DAB Peroxidase Substrate kit (Vector Labs Inc, Burlingame, CA).

Real-time RT-PCR measurements of viral titers: The number of viral RNA copies was measured using quantitative real-time reverse-transcription PCR (73,74). RNA was extracted from H1N1-infected lung tissue using a SurePrep TrueTotal RNA Purification Kit (Fisher Scientific, Fair Lawn, NJ). RNA (1 µg) was reverse transcribed into cDNA using a High-Capacity cDNA Reverse Transcription Kit (ThermoFisher Scientific, Carlsbad, CA). Quantitative PCR was performed to amplify H1N1 cDNA using AriaMx Real-Time PCR machine (Agilent technologies, Santa Clara, CA) and primers (ThermoFisher Scientific, Waltham, MA) for H1N1 IAV (5' to 3' H1N1 forward primer TTCACAGCATCGGTCTCACAGACA H1N1 reverse primer TCCAGCCATCTGTTCCATAGCCTT) and β-actin (β-actin forward primer AGTGTGACGTTGACATCCGT and β-actin reverse primer TGCTAGGAGCCAGAGCAGTA) as the housekeeping gene (**Supplemental Table 2**). The number of copies of H1N1 cDNA was calculated using H1N1 DNA standards of known concentration.

Lymphocyte subset enumeration in enzymatic lung digests: The following antibodies were used: rat anti-CD25 IgG2b conjugated to FITC, rat anti-CD8 IgG1 conjugated to FITC or APC-Cy7, murine anti-Foxp3 IgG1 conjugated to PE, rat anti-B220 IgG2a conjugated to PerCP, rat anti-murine CD90.2 IgG2b conjugated to PerCP, rat anti-CD366 (Tim3) IgG2a conjugated to PE, rat anti-PD1 IgG2a conjugated to APC, murine anti-CD45 IgG2a conjugated to APC/Cy7 or AlexaFluor 700, rat anti-CD4 IgG2b conjugated to PE/Cy7 or FITC, murine anti-NK-1.1 IgG2a conjugated to PE or APC, armenian hamster anti-δγT cell receptor

conjugated to APC, armenian hamster anti-TCR- β chain conjugated to Brilliant Violet 421™. After gating on live CD45⁺ cells, lymphocyte populations were identified as follows: a) CD4⁺ T cells (CD90.2⁺ and CD4⁺); b) CD8⁺ T cells (CD90.2⁺ and CD8⁺); c) Tregs (CD90.2⁺, CD4-PE⁺, Foxp3⁺); d) B cells (B220⁺ CD90.2⁻) e) CD8⁺ T cell subsets gated by PD1 and CD366. Double negative (DN) populations were sub-classified as: a) NKT cells (NK1.1⁺ and TCR β ⁺); b) NK cells (NK-1.1⁺ TCR β ⁻); and c) $\gamma\delta$ T cells (TCR $\gamma\delta$ ⁺). Flow cytometry was performed on a BD LSR Fortessa Cell Analyzer (San Jose, CA) and analyzed with FlowJo software (Tree Star, Inc).

Respiratory mechanics: Respiratory mechanics were measured on anesthetized mice 7 days after they were infected with a LD₂₀ inoculum of H1N1 by the intranasal route as described previously (5). See online supplement for details. Mice were anesthetized using a mixture of ketamine (100 mg/kg), xylazine (10 mg/kg), and acepromazine (3 mg/kg). A tracheal cannula was inserted, and connected each mouse to a FlexiVent device [a digitally-controlled mechanical ventilator (Scireq Inc., Montreal, Quebec, Canada)]. The ventilator was set for $f = 150/\text{min}$, $\text{FiO}_2 = 0.21$, tidal volume = 10 ml/kg body weight, and a positive end-expiratory pressure (PEEP) of 3 cm of H₂O. Tissue elastance and peripheral airway elastance were measured at a PEEP of 3 cmH₂O, followed by stepwise quasi-static compliance (C_{st}), and volume-pressure flow curves (5). The mice were then humanely euthanized.

Infection of differentiated human bronchial epithelial cells (HBECs) and measurement of transepithelial electrical resistance: HBECs were isolated from human lung tissue obtained from the organ and tissue donation program of the International Institute for the Advancement of Medicine using a published method (6). Cells were grown in monolayers, transferred to 6.5 mm diameter transwells (0.4 μm pore size), and differentiated at an air-liquid interface (ALI) using Lonza tissue culture reagents (Lonza Group, Basel, Switzerland) for bronchial epithelial cell growth and differentiation following the manufacturer's protocol.

Cellular differentiation was enhanced, following exposure of the cells to air, by adding 10 nM recombinant human *neuregulin-1α*/epidermal growth factor-like domain of heregulin- α (296-HR-050, R&D Systems, Minneapolis, MN) to the basolateral media. After ~2 weeks of exposure to air, the HBECs demonstrated hallmarks of cellular differentiation (mucus production and the appearance of cilia). HBECs were infected with H1N1 at ~0.01-0.6 MOI (400-27,000 PFU/transwell). At intervals thereafter, apical surfaces were washed 3 times with 200 μ L of PBS to measure viral titers, as described above for murine lung samples. Cell monolayers were lysed in TRIzol® LS Reagent (ThermoFisher Scientific, Waltham, MA) to isolate RNA for gene expression studies. HBECs were infected with H1N1 (MOI 0.1) and transepithelial electrical resistance (TEER) (7) was measured to determine the barrier integrity using EVOM² Epithelial Voltohmeter with an Electroset for EVOM (electrode model STX3; Sarasota, FL).

Assessment of cleavage of viral proteins by MMP-9: To determine whether MMP-9 degrades H1N1 viral proteins, human proMMP-9 (EMD Millipore, Billerica, MA) was activated in Tris assay buffer (50 mM Tris, 0.15 M NaCl, 0.02 M CaCl₂, and 0.05% Brij 35; pH 7.4) by adding 1 mM of 4-aminophenylmercuric acetate (APMA) (Sigma-Aldrich, St Louis, MO) and incubating the solution at 37°C for 3 h (12). Activation of MMP-9 was confirmed by incubating 10 nM of the APMA-activated MMP-9 with 2 μ M Mca-PLGLDpa-AR (Calbiochem, San Diego, CA), a sensitive, quenched, fluorogenic substrate for MMP-9, and qualifying cleavage of the substrate with a fluorimeter, as described previously (8). Recombinant hemagglutinin (HA1) and neuraminidase (NA1) from Influenza A/California/07/2009 H1N1 were obtained from BEI Resources (Manassas, VA). HA1 (100 nM) or NA1 (1000 nM) were incubated in Tris assay buffer overnight at 37°C, with or without 30 nM active MMP-9, in the presence or absence of a non-selective MMP inhibitor 1,10-phenanthroline (1 mM; Sigma-Aldrich, St Louis, MO). The reaction was stopped by adding Laemmli sample buffer (Bio-Rad Laboratories, Hercules, CA) containing β -mercaptoethanol (Sigma-Aldrich, St Louis, MO). Reaction products were separate

on 12% SDS-PAGE gels and visualized by silver staining of gels using a commercial kit (ThermoFisher Scientific, Waltham, MA). The silver stained bands were excised and cleavage products were sequenced by the proteomics Core at the Whitehead Institute for Biomedical Research (Cambridge, MA).

Supplemental Table 1: PROSPER results for cleavage prediction analysis of hemagglutinin subunit 1 and neuraminidase subunit 1 by human MMP-9.

Hemagglutinin subunit 1 Protein				
Position	P4-P4' site	NH₃-terminal fragment (kDa)	COOH terminal fragment (kDa)	Cleavage score
147	FYKN LIWL	17.25	21.32	1.25
199	DAYV FVGS	23.49	15.08	1.23
297	NIHP ITIG	35.02	3.55	1.11
256	YAFAMERN	30.31	8.26	1.11
317	LATG LRNI	37.41	1.16	1.1
31	HSVN LLED	3.45	35.12	1.09
284	TPKG AINT	33.59	4.98	1.08
247	ATGN LVVP	29.3	9.27	1.06
49	GVAP LHLG	5.66	32.91	1.04
19	VDTV LEKN	2.13	36.44	1.01
43	KLCK LRGV	4.95	33.62	0.99
Neuraminidase subunit 1 Protein				
Position	P4-P4' site	NH₃ terminal fragment (kDa)	COOH terminal fragment (kDa)	Cleavage score
307	VSFN QNLE	36.33	20.42	1.19
169	VPSP YNSR	19.82	36.94	1.17
372	NGFE MIWD	44.64	12.12	1.17
309	FNQN LEYQ	36.58	20.18	1.15
5	NPNQ KIIT	0.58	56.18	1.14
21	GMAN LILQ	2.44	54.31	1.13
273	NAPN YHYE	32.15	24.6	1.1
466	LPFT IDK	56.41	0.35	1.09
18	MTIG MANL	2.13	54.63	1.08
241	CFTV MTDG	28.32	28.44	1.07
28	QIGN IISI	3.31	53.44	1.07
171	SPYN SRFE	20.09	36.66	1.05
67	QTYV NISN	7.96	48.8	1.04
425	FWVE LIRG	51.38	5.38	1.02
248	GPSN GQAS	29.13	27.62	1.02
53	NQSV ITYE	6.23	50.52	1.01
209	LKYN GIIT	24.54	32.21	0.98
205	AVAV LKYN	24.03	32.73	0.95
379	DPNG WTGT	45.57	11.19	0.95
254	ASYK IFRI	29.88	26.87	0.92

Using the PROtease substrate SPecificity servER (PROSPER) for cleavage predication analysis (9), we predicted that MMP-9 cleaves both hemagglutinin subunit 1 (HA1) and neuraminidase subunit 1 (NA1) at multiple cleavage sites, generating multiple possible fragments having different molecular weights. The predicted residue and the amino acid sequence around the cleavage site, the molecular weight of the predicted NH₃- and COOH-terminal fragments, and the cleavage score (which represents the probability of cleavage in a particular site within the substrate protein) are shown in the Table.

Supplemental Table 2: Sequences of the primers used for real time PCR analysis of *MMP-9* and *H1N1 IAV* gene expression in epithelial cell cultures

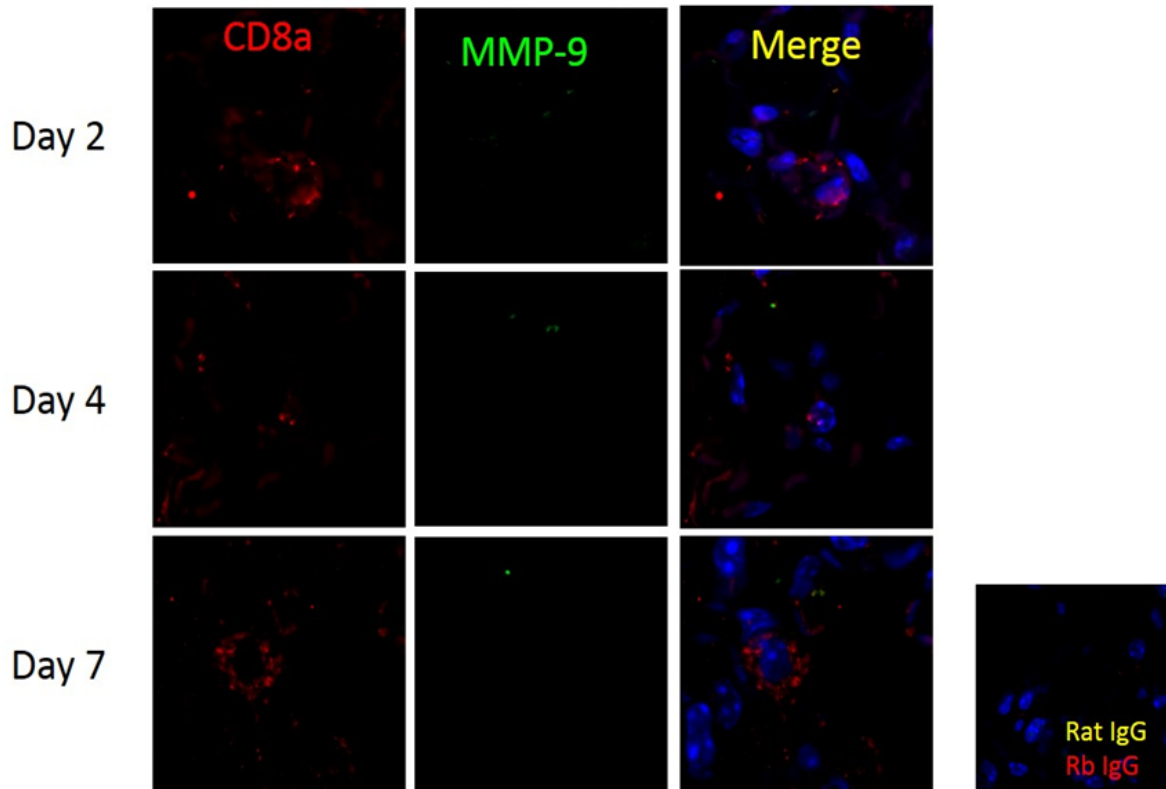
2009 H1N1 (M-gene)*	5'-TTCACAGCATCGGTCTCACAGACA-3' forward
	5'-TCCAGCCATCTGTTCCATAGCCTT-3' reverse
	5' FAM-AACAGAATGGTGCTGGCTAGCACT BHQ1-3' probe
RNase P (human)§	5'-AGATTTGGACCTGCGAGCG-3' forward
	5'-GAGCGGCTGTCTCCACAAGT-3' reverse
	5' HEX-TTCTGACCTGAAGGCTCTGCGCG BHQ1-3' probe

*Sequences of the Taqman primers used to perform real time qPCR analysis of *H1N1* gene expression.

§RNase P was used as the housekeeping control gene.

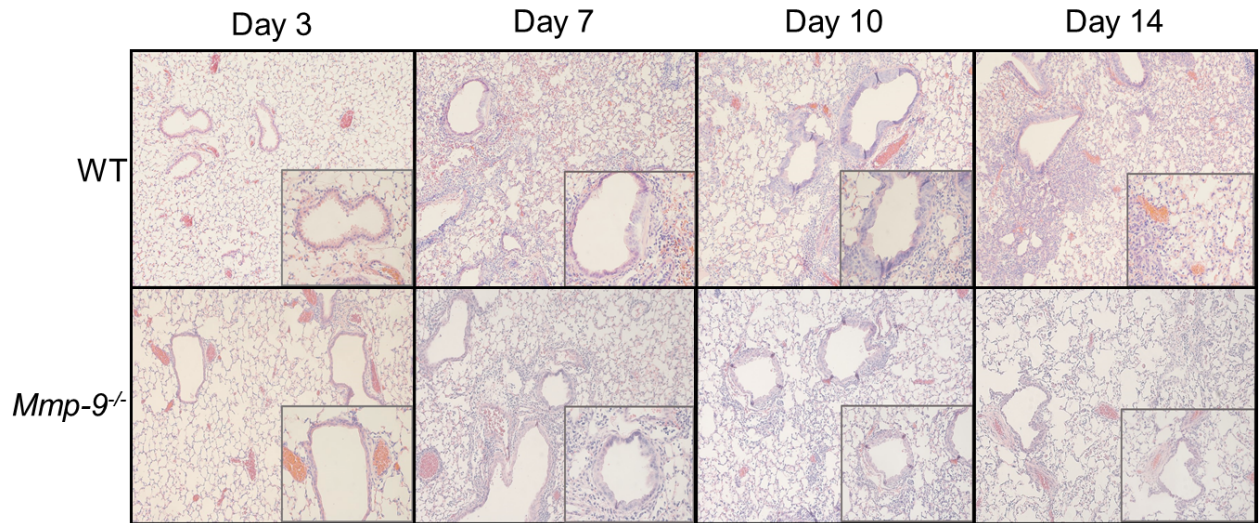
The comparative threshold method was used to measure *H1N1* gene expression.

Supplemental Fig. 1



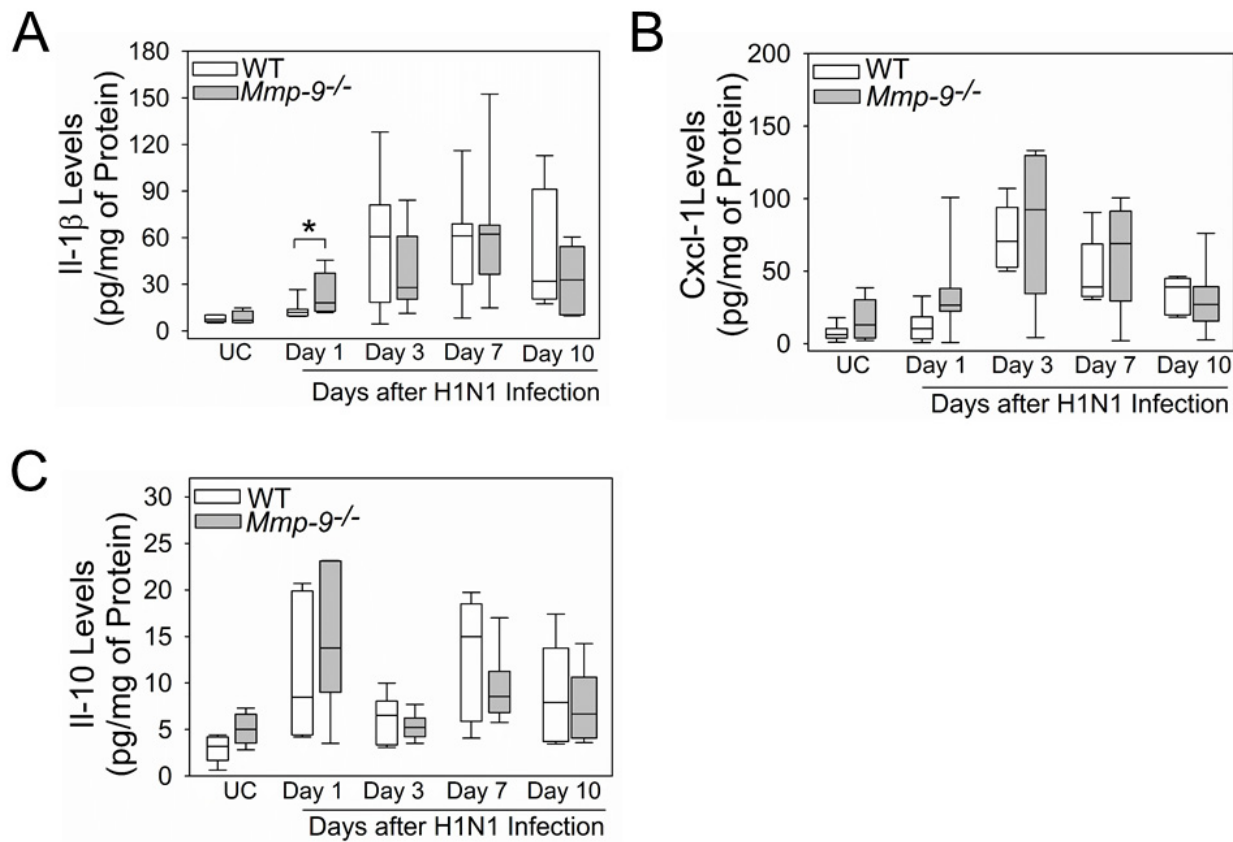
Supplemental Fig. 1. *Mmp-9 is not up-regulated in CD8+ T cells recruited into IAV infected lungs:* WT mice were infected with a LD₂₀ inoculum of A/California/07/2009 H1N1 strain IAV by the intranasal route, or not infected as a control. Lung sections from the mice were double immunostained with a green fluorophore for Mmp-9 and a red fluorophore for CD8a. Nuclei were counterstained blue with 4',6-diamidino-2-phenylindole. Immunostained lung sections were examined with a confocal microscope and merged images are shown in the right panels. The lungs of infected mice were also stained with non-immune isotype-matched primary antibodies [rabbit (Rb) IgG or rat IgG], and images of these sections are shown in the far right panel. Images shown are representative of sections from 5 mice per experimental group. Magnification is X 400.

Supplemental Fig. 2



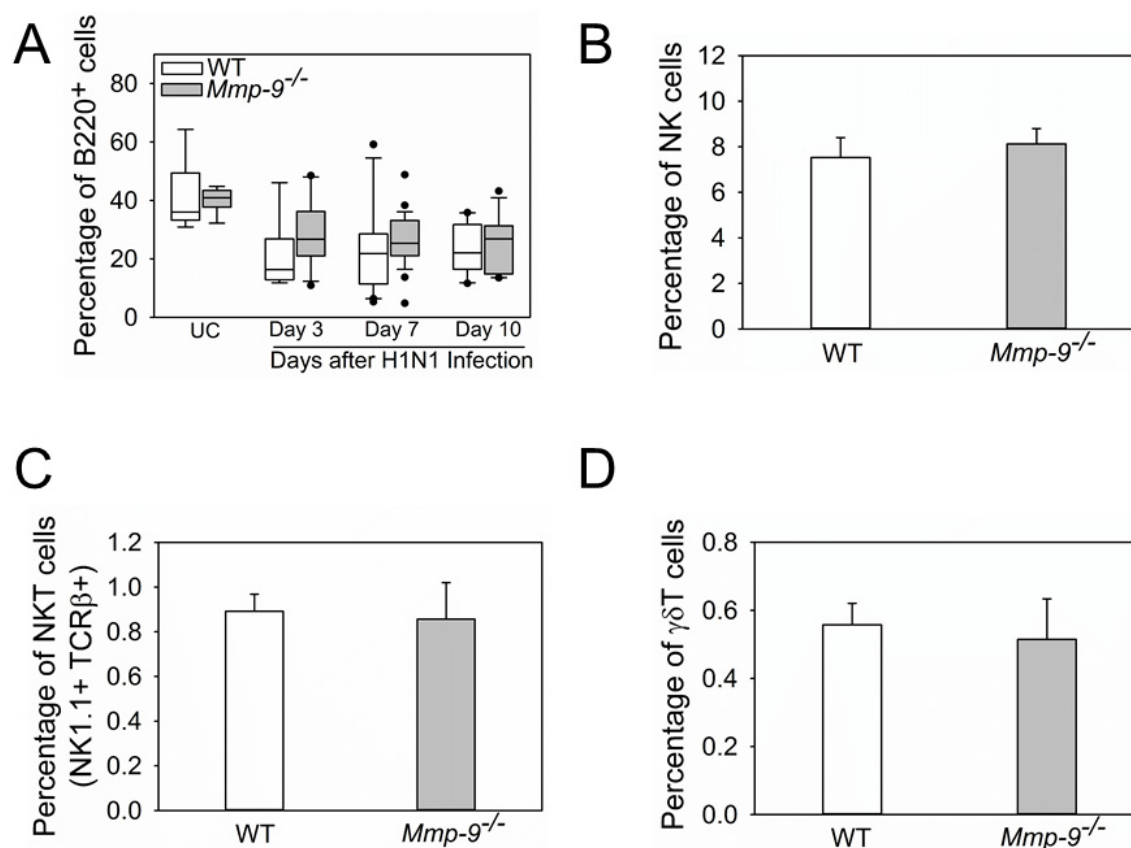
Supplemental Fig. 2. *Mmp-9^{-/-}* mice have reduced histopathologic changes in their lungs following H1N1 infection: WT and *Mmp-9^{-/-}* mice were infected with a LD₂₀ inoculum of H1N1 by the intranasal route. At indicated intervals p.i., lung sections were stained with hematoxylin and eosin. The images are representative of 5 mice/group. Magnification is X 100. Insets show areas of airway/parenchymal inflammation at a higher magnification (X 400) that are representative of 5 mice per group. Uninfected WT and *Mmp-9^{-/-}* mice had no lung inflammation (not shown).

Supplemental Fig. 3



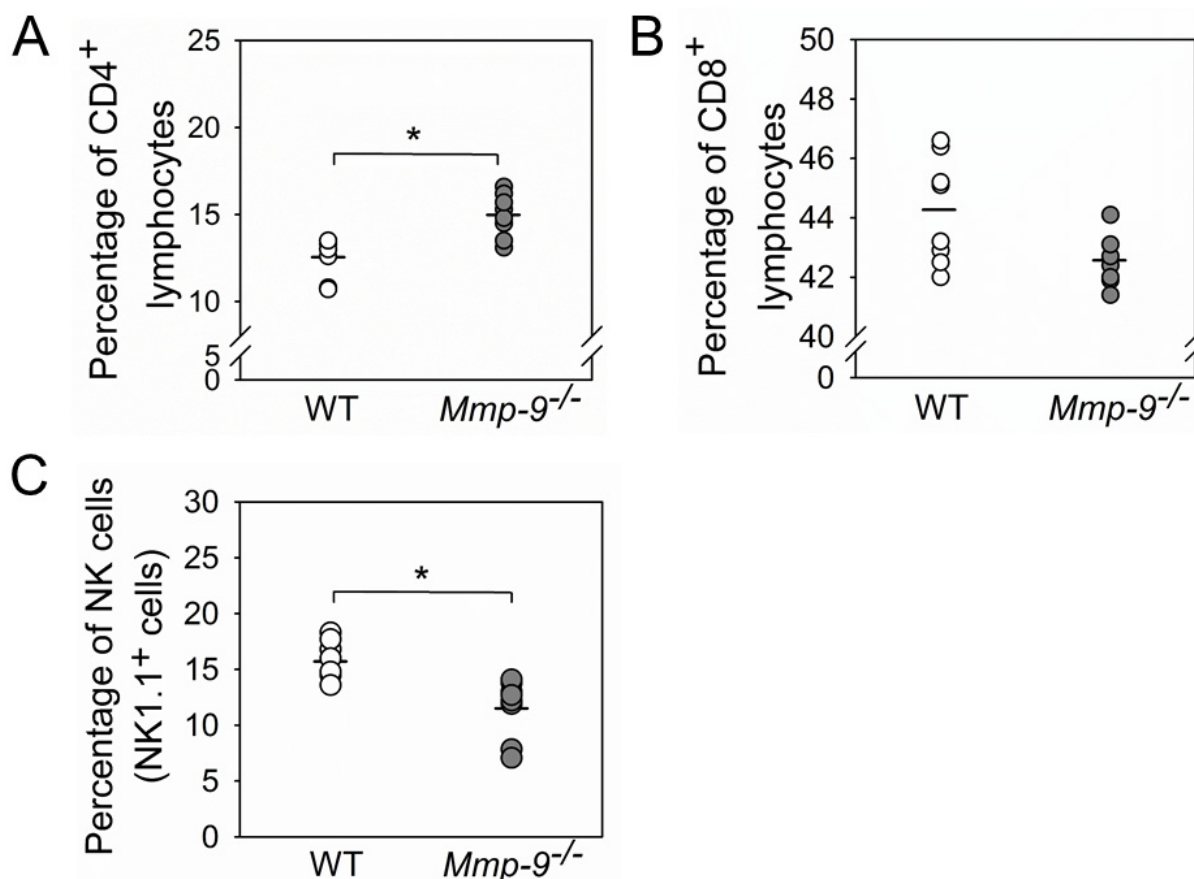
Supplemental Fig. 3. *Mmp-9*^{-/-} mice have similar lung levels of IL1- β , Cxcl-1, and IL-10: WT mice and *Mmp-9*^{-/-} mice (4-10 mice per experimental condition) were infected with LD₂₀ inoculum of A/California/07/2009 H1N1 strain IAV, or not infected (UC) as a control. At intervals post infection (p.i.), levels of IL1- β , Cxcl-1, and IL-10 were measured in homogenates of lungs using ELISAs and lung levels of mediators were normalized to lung total protein levels. Compared with IAV-infected WT mice, IAV-infected *Mmp-9*^{-/-} mice had higher lung levels of IL-1 β only on day 3 p.i. (**A**). IAV-infected WT and *Mmp-9*^{-/-} mice had similar levels of Cxcl-1 (**B**) and IL-10 (**C**) at all time-points measured. The box-plots show the medians and 25th and 75th percentiles, and the whiskers show the 10th and 90th percentiles. Data were analyzed with one-way ANOVAs. Data were analyzed with one-way ANOVAs followed by pair-wise testing with Mann-Whitney U tests. Asterisks indicate $P < 0.05$.

Supplemental Fig. 4



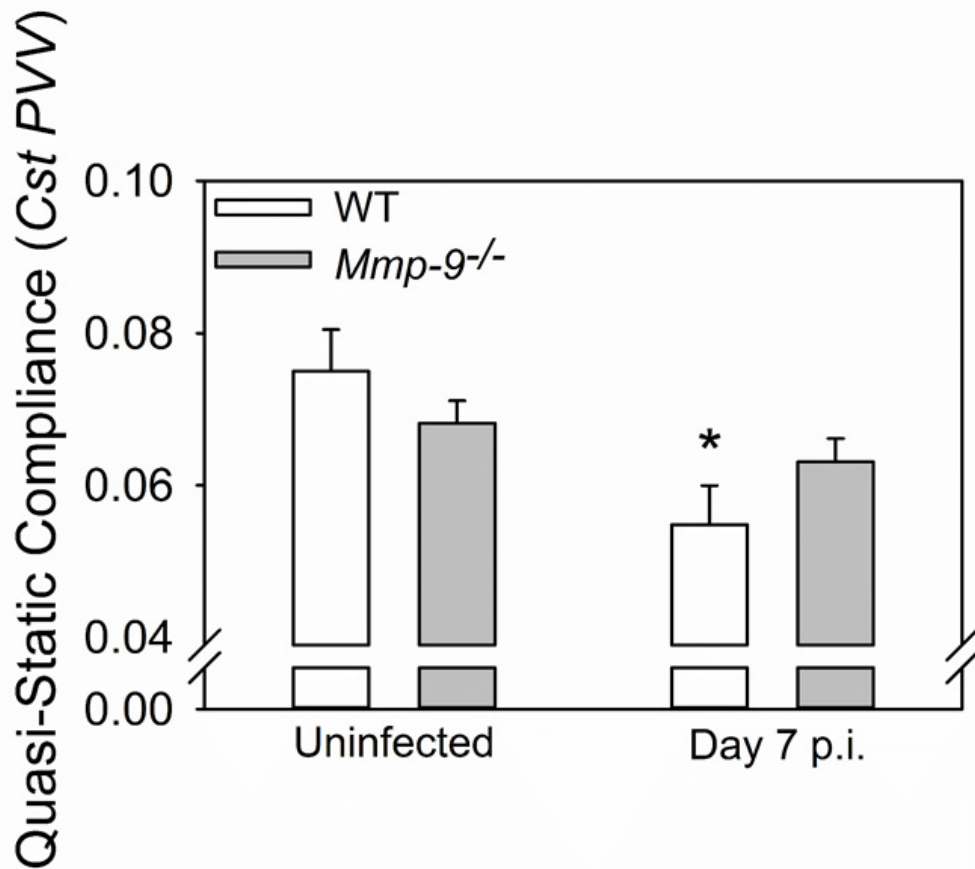
Supplemental Fig. 4. IAV infected WT and *Mmp-9*^{-/-} mice have similar B cells, NK cells, NKT cells, and $\delta\gamma$ T cell counts in their lungs. WT and *Mmp-9*^{-/-} mice were infected with a LD₂₀ inoculum of A/California/07/2009 H1N1 strain IAV by the intranasal route. At intervals post infection, lungs were removed and enzymatically digested. Uninfected (UC) mice served as controls. Lung cells were immunostained for markers of leukocytes (CD45⁺), B cells (B220⁺), NK (NK1.1⁺), NKT (NK1.1⁺ TCRβ⁺) cells, and $\delta\gamma$ T cells. The frequencies of these leukocyte subsets were quantified in the CD45⁺ population using flow cytometry. **Panel A** shows the frequencies of B cells in the lung digests. The box-plots show the medians and 25th and 75th percentiles, and the whiskers show the 10th and 90th percentiles. Data were analyzed with one-way ANOVAs followed by pair-wise testing with Mann-Whitney U tests. In **B-D**, the frequencies of CD45⁺ leukocytes that were NK cells (**B**), NKT cells (**C**) and $\delta\gamma$ T cells (**D**) were quantified in digests of lungs harvested on day 7 p.i. were measured using mean \pm SEM values. Data were analyzed with one-way ANOVAs followed by 2-sided Student's t-tests. There were no significant differences between WT and *Mmp-9*^{-/-} mice for any of the leukocyte subsets studied.

Supplemental Fig. 5



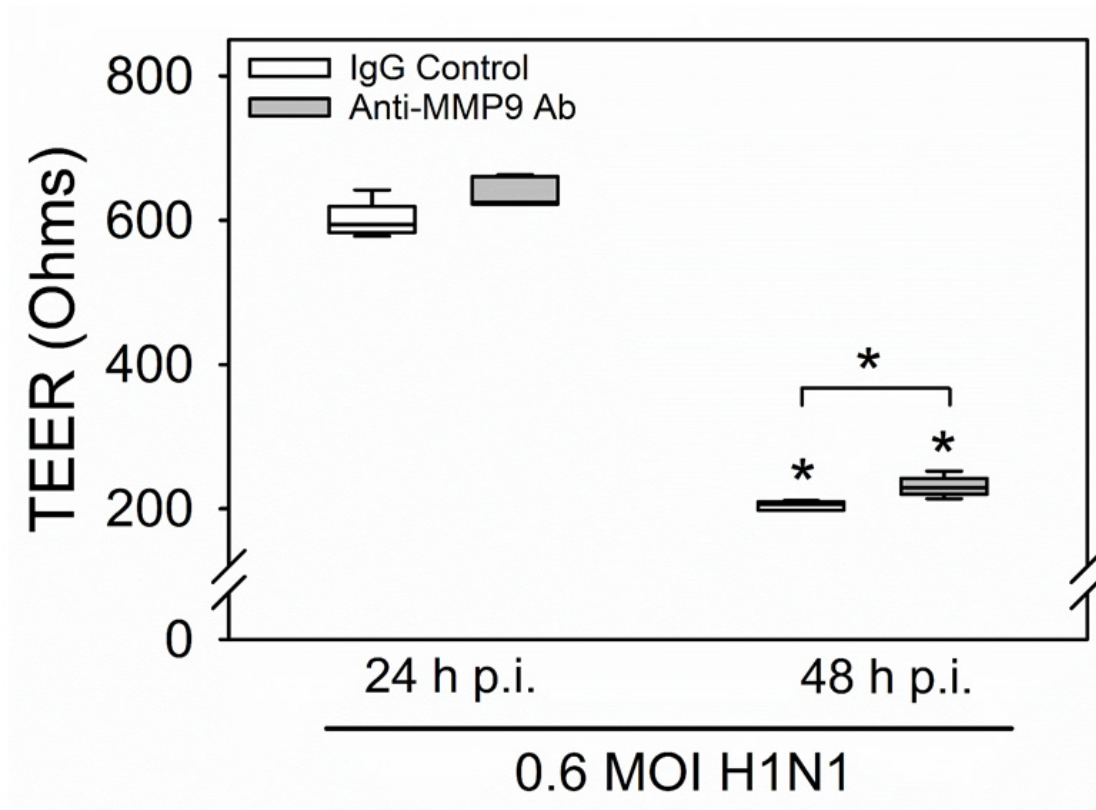
Supplemental Fig. 5. H1N1-infected *Mmp-9*^{-/-} mice have higher BAL CD4⁺ lymphocytes and lower BAL NK cells than H1N1-infected WT mice: WT and *Mmp-9*^{-/-} mice infected with a LD₂₀ inoculum of H1N1 via the intranasal route. Bronchoalveolar lavage (BAL) was performed on day 7 p.i. (8 mice per group). BAL leukocytes were immunostained for markers of CD4⁺ T cells (A), CD8⁺ T cells (B), and NK (NK1.1⁺) cells (C) and analyzed using flow cytometry. In A and C, the mean is indicated as a horizontal line in each plot. Data were analyzed with one-way ANOVAs followed by 2-sided Student's t-tests. Asterisks indicate $P < 0.05$. In B, the median is indicated as a horizontal line in each plot. Data were analyzed with one-way ANOVAs followed by 2-sided Mann-Whitney U.

Supplemental Fig. 6



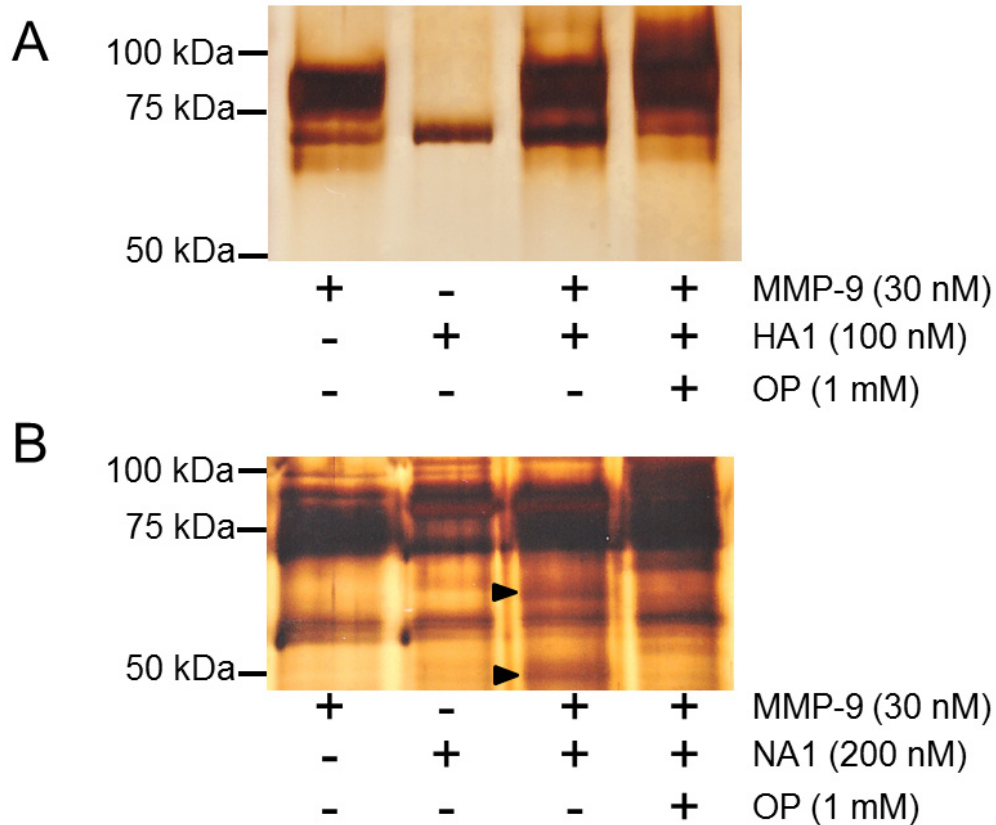
Supplemental Fig. 6. Unlike H1N1-infected WT mice, H1N1-infected *Mmp-9^{-/-}* mice are protected from H1N1-induced reductions in quasi-static lung compliance. WT and *Mmp-9^{-/-}* mice were infected with a LD₂₀ inoculum of H1N1 by the intranasal route. Uninfected mice served as controls. Quasi-static compliance (**D**) was measured using a FlexiVent device on H1N1-infected mice on day 7 p.i. (8 mice per group) and uninfected control mice (8-9 mice per group). Data are mean ± SEM. Data were analyzed with one-way ANOVAs followed by 2-sided Student's t-tests. Asterisk indicates $P = 0.02$ between uninfected and IAV-infected WT mice. There was no significant difference in quasi-static lung compliance between uninfected and IAV-infected *Mmp-9^{-/-}* mice ($P = 0.257$).

Supplemental Fig. 7



Supplemental Fig. 7: A neutralizing antibody to MMP-9 modestly attenuates IAV-induced reductions in trans-epithelial electrical resistance (TEER). Murine tracheal epithelial cell monolayers were infected 0.6 MOI of A/California/07/2009 H1N1 strain IAV, and after 24 and 48h TEER was measured, as described in Methods. The box-plots show medians and 25th and 75th percentiles, and the whiskers show the 10th and 90th percentiles (n = 10/group). Data were analyzed with one-way ANOVAs followed by pairwise comparisons using Mann-Whitney U tests. Asterisks indicate $P < 0.05$ versus the group indicated or the same experimental condition at the 24 h time-point.

Supplemental Fig. 8



Supplemental Figure 8: MMP-9 does not cleave HA1 hemagglutinin or neuraminidase protein in vitro: **A:** Purified hemagglutinin subunit 1 (HA1; 100 nM) was incubated at 37°C for 18 h with or without 30 nM active human MMP-9, in the presence or absence a non-selective metalloproteinase inhibitor (1 mM 1,10-phenanthroline [OP]). Reaction products were separated and visualized on silver stained 12% SDS-PAGE gels. Note the lack of reduction in the intensity of the band corresponding to intact HA1 and the absence of lower molecular weight HA1 cleavage products when HA1 is incubated with active MMP-9. The results shown are representative of 3 separate experiments. **B:** Purified neuraminidase subunit 1 (NA1) protein (200 nM) was incubated at 37°C for 18 h with or without 30 nM active human MMP-9, in the presence or absence a non-selective metalloproteinase inhibitor (1 mM 1,10-phenanthroline [OP]). Residual intact viral proteins and cleavage products were separated and visualized on silver stained 12% SDS-PAGE gels. Arrow heads indicate NA1 cleavage products generated. The very small amounts of cleavage products generated at the enzyme to substrate ratio tested (1:6.7) is very unlikely to be of any biologic significance. The results shown are representative of 3 separate experiments.

References

1. Betsuyaku T, Shipley JM, Liu Z, Senior RM. Gelatinase B Deficiency Does Not Protect Against Lipopolysaccharide-Induced Acute Lung Injury. *Chest* 1999;116 (1 Suppl):17S-18S.
2. Neutrophil Emigration in the Lungs, Peritoneum, and Skin Does Not Require Gelatinase B. *Am J Respir Cell Mol Biol* 1999;20:1303-1309.
3. Knolle MD, Nakajima T, Hergueter A, Gupta K, Polverino F, Craig VJ, Fyfe SE, Zahid M, Permaul P, Cernadas M, et al. Adam8 Limits the Development of Allergic Airway Inflammation in Mice. *J Immunol* 2013;190:6434-6449.
4. Craig VJ, Quintero PA, Fyfe SE, Patel AS, Knolle MD, Kobzik L, Owen CA. Profibrotic Activities for Matrix Metalloproteinase-8 During Bleomycin-Mediated Lung Injury. *J Immunol* 2013;190:4283-4296.
5. Laucho-Contreras ME, Taylor KL, Mahadeva R, Boukedes SS, Owen CA. Automated measurement of pulmonary emphysema and small airway remodeling in cigarette smoke-exposed mice. *J Vis Exp* 2015;95:52236.
6. Fulcher ML, Gabriel S, Burns KA, Yankaskas JR, Randell SH. Well-Differentiated Human Airway Epithelial Cell Cultures. *Methods Mol Med* 2005;107:183-206.
7. Srinivasan B, Kolli AR, Esch MB, Abaci HE, Shuler ML, Hickman JJ. TEER Measurement Techniques for in Vitro Barrier Model Systems. *J Lab Autom* 2015;20:107-126.
8. Owen CA, Hu Z, Barrick B, Shapiro SD. Inducible Expression of Tissue Inhibitor of Metalloproteinases-Resistant Matrix Metalloproteinase-9 on the Cell Surface of Neutrophils. *Am J Resp Cell Mol Biol* 2003;29:283-294.

9. Song J, Tan H, Perry AJ, Akutsu T, Webb GI, Whisstock JC, Pike RN. PROSPER: an Integrated Feature-Based Tool for Predicting Protease Substrate Cleavage Sites. *PLoS ONE* 2012;7:e50300.